

## Research Article

# Gecko Crude Peptides Induce Apoptosis in Human Liver Carcinoma Cells *In Vitro* and Exert Antitumor Activity in a Mouse Ascites H22 Xenograft Model

Ying Song,<sup>1,2</sup> Jian-Gang Wang,<sup>1</sup> Rui-Fang Li,<sup>1</sup> Yan Li,<sup>1</sup> Zhao-Chu Cui,<sup>1</sup>  
Leng-Xin Duan,<sup>1</sup> and Fei Lu<sup>2</sup>

<sup>1</sup>Medical College, Henan University of Science & Technology, Luoyang 471003, Henan Province, China

<sup>2</sup>The 1st Affiliated Hospital of Henan University of Science and Technology, Luoyang 471003, Henan Province, China

Correspondence should be addressed to Jian-Gang Wang, ylwjg@163.com

Received 28 May 2012; Revised 17 August 2012; Accepted 22 August 2012

Academic Editor: Kazim Husain

Copyright © 2012 Ying Song et al. This is an open access article distributed under the Creative Commons Attribution License, which permits unrestricted use, distribution, and reproduction in any medium, provided the original work is properly cited.

**Aim.** To investigate the anti-tumor effects and mechanisms of gecko crude peptides (GCPs) *in vitro* and *in vivo*. **Methods.** 3-(4,5)-dimethylthiazoliazolo (-z-y1)-3,5-di-phenyltetrazoliumromide (MTT) assay was applied to measure the effects of GCPs on the HepG2 cell viability. Fluorescence morphology was used to identify apoptotic cells. A xenograft H22 liver cancer model was established in Kunming mice. The tumor-bearing mice were treated with daily intraperitoneal injections of normal saline (NS group) or GCPs (80, 40 or 20 mg/kg) for 10 days, or once per two days with 2 mg/kg doxorubicin (ADR group;  $n = 10$  each). Serum tumor necrosis factor (TNF- $\alpha$ ) and interleukin (IL)-6 were quantified using ELISA assay. **Results.** GCPs significantly inhibited the growth of HepG2 cells and induced typical apoptotic morphological features through increasing bcl-2/bax ratio in a dose- and time-dependent manner *in vitro*. The tumor weights of the ADR group, GCPs (H) group, GCPs (M) group, GCPs (L) group were smaller compared to the NS group. While the white blood cell count, thymus index, spleen index were higher in the high dose GCPs group than the NS group ( $P < 0.05$ ), the VEGF expression in tumor tissue and serum TNF- $\alpha$  and IL-6 levels in the GCPs groups were lower than the NS group ( $P < 0.05$ ).

## 1. Introduction

Cancer has a major impact on human health. Many current chemotherapeutic drugs are cytotoxic and lead to numerous side effects [1, 2]; therefore, Chinese *materia medica* is increasingly being used for its antitumor effects. The small peptides from snake venom of *Gloydus saxatilis* and scorpion venom have antitumor activities and upregulate the immune system in a dose-dependent manner [3–8].

Gecko is an animal, which can reduce inflammation, allergic responses swelling [9, 10], with a high activity and low toxicity, which has been used in Chinese medicine for a long time, Gecko has a proven effect against malignant tumors in clinical practice, especially digestive system tumors such as esophageal cancer, gastric cancer, and liver cancer [11–13]. Pharmacological studies reveal that Gecko represents a variety of activities, such as the cytotoxic effects

and induction of apoptosis [9, 10]. The aim of this study was to purify and further separate Gecko alcohol extract (GAE) to obtain Gecko crude peptides (GCPs), to investigate the antitumor effect and mechanism of action of GCPs on HepG2 cells *in vitro* and in a mouse xenograft model of ascites H22 tumors.

## 2. Materials and Methods

**2.1. Reagents.** Whole-dried *Gekko japonicus* (Anhui Bozhou Yonggang Co. Ltd., Bozhou, China) were ground to a fine powder and further separated in Gecko alcohol extract (GAE) to obtain Gecko crude peptides (GCPs), which were then desalted and dialyzed. The human liver carcinoma cell line HepG2 and the H22 mouse cell line were kindly provided by the Medical College of Zhengzhou University; 5-Fluorouracil (5-Fu; batch no. H110911) was purchased from

Shanghai Xudong Medicine Co. Ltd, China; doxorubicin (ADR; batch no. H090303A) was purchased from Zhejiang Haizheng Medicine Co. Ltd., China. RPMI-1640 and calf serum were purchased from Invitrogen Inc. (Carlsbad, CA, USA); trypsin, all other cell culture reagents and Hoechst 33258 (Batch no. 861405) were obtained from Sigma-Aldrich Inc. (St. Louis, MO, USA). The antibodies used for Western blotting were purchased from Cell Signaling Technology, Inc. (Boston, MA, USA). Fifty female Kunming mice (Code number 0001350) were provided by the Medical Experimental Animal Center, Henan Province, China. The mouse TNF- $\alpha$  and IL-6 ELISA kits were purchased from NeoBioscience Technology Co., Ltd., Beijing, China. All other reagents, of at least analytical grade purity, were obtained from Sigma-Aldrich Inc.

## 2.2. In Vitro Study

**2.2.1. Cell Culture.** The cells were cultured as monolayers in RPMI-1640 media supplemented with 10% fetal calf serum, 100 U/mL penicillin and 100 mg/L streptomycin in humidified air containing 5% CO<sub>2</sub> at 37°C.

**2.2.2. 3-(4, 5-Dimethylthiazol-2-yl)-2,5-Diphenyltetrazolium Bromide (MTT) Assay.** Cell growth was measured using a modified MTT assay [14–16]. HepG2 cells in the populations growth were resuspended in 0.02% (w/v) EDTA at  $1 \times 10^4$  cells/mL, and 180  $\mu$ L aliquots were plated in 96-well plates and cultured for 24 h. Three groups of six wells were prepared: control group, 5-Fu group (1.3 mg/mL) and the Gecko groups (3, 1.5, 1, 0.75, and 0.375 mg/mL). Each well was treated with 20  $\mu$ L complete media containing drugs as indicated, incubated for 24, 48, or 72 h, then 20  $\mu$ L MTT was added to each well and incubated at 37°C for 4 h. The supernatant was removed, 200  $\mu$ L DMSO was added to each well to solubilize the formazan product, then the absorbance (A; aka the OD value) was measured at 470 nm using a microplate reader (Sigma). Triplicate experiments were performed in a parallel manner for each concentration and the mean  $\pm$  SD values were calculated. The cell inhibitory rate (IR%) was calculated as  $IR\% = (1 - A_{\text{treated}}/A_{\text{control}}) \times 100\%$ .

**2.2.3. Morphological Assessment and Quantification of Apoptotic Cells.** Variations in cell morphology were analyzed by fluorescence microscopy. Cells attached to coverslips were fixed in cold methanol for 5 min, air dried, and stained with Hoechst 33258 (2.5 mg/mL in distilled water) for 2 min [14, 15]. Microscopic observations were carried out using an Olympus BX41 microscope and photographs were taken with an Olympus A640 digital camera.

**2.2.4. Western Blotting.** HepG2 cells were seeded at a density of  $1 \times 10^5$  cells/mL in 25 cm<sup>2</sup> culture flasks, incubated with different concentrations of GCPs for 48 h, washed twice in ice-cold PBS, and harvested by scraping into 1 mL Tris-Tricine-SDS buffer. Tumor tissues were homogenized in lysis buffer containing proteinase inhibitors.

Western blotting was performed as previously described [14, 17, 18]. Briefly, after protein quantitation using a modified Bradford assay, 80  $\mu$ g protein was boiled in loading buffer and then loaded onto gradient sodium dodecyl sulphate-polyacrylamide gels. Following electrophoresis, proteins were transferred to a polyvinylidene difluoride membrane at 100 V/350 mA for 60 min. The anti-bcl-2 and anti-bax polyclonal antibody were used as primary antibody. The antibody exhibits immunoreactivity against both the full-length and the cleaved fragment of bcl-2 and bax. For detection of VEGF, monoclonal VEGF antibody was used. Images were analyzed with Gel Analyzer (Media Cybernetics, USA).

## 2.3. In Vivo Study

**2.3.1. Establishment of the H22 Xenograft Model.** The H22 model was established by subcutaneous injection as previously described [13]. Briefly, H22 mouse cells were harvested with ascites, diluted 1:8 in sterile saline, the cell concentration was adjusted to  $1.0 \times 10^6$  cells/mL, and the cells were subcutaneously inoculated into the right armpit region of Kunming mice ( $n = 50$ ; 8–10 weeks old, weighing  $22 \pm 2$  g). In the experiment, the mouse was anesthetized by ether. All experimental procedures were performed in accordance with the Guide lines of Animal Experiments from the Committee of Medical Ethics, National Health Department of China (1998).

**2.3.2. Inhibitory Effect of GCPs on H22 Tumor Xenografts.** Twenty-four hours after establishment of the H22 model, the transplanted mice were randomly divided into five groups: the normal saline (NS) group, the ADR group (ADR is frequently used as a positive control as it has a cytotoxic effect against mouse H22 [9, 10, 13]) and the Gecko groups. The mice were treated with a daily peritoneal injection of saline, single peritoneal injection of 100 mg/kg ADR, or daily peritoneal injection of 80, 40, or 20 mg/kg GCPs. After 10 days, the antitumor activity was evaluated by weighing the tumor tissues. The tumor inhibitory rate (%) was calculated as  $(1 - \text{average tumor weight} / \text{average tumor weight of NS group}) \times 100\%$ .

**2.3.3. Immune Function Analysis.** Blood was collected from the mouse eye orbit, followed by diluted with 2% acetate (acetic acid), and the white blood cell count was determined by microscopy. The thymus and spleen were taken from the mice and the impact of the treatments on immune organ function was evaluated using the thymus index and spleen index [9]. Spleen index =  $\text{spleen weight(g)} / \text{body weight(10 g)} \times 100\%$ , thymus index =  $\text{thymus weight(g)} / \text{body weight(10 g)} \times 100\%$ .

**2.3.4. Enzyme-Linked Immunosorbent Assay (ELISA).** The serum was diluted to different concentrations and analyzed using the mouse TNF- $\alpha$  and IL-6 ELISA kits, following the manufacturer's instructions.

TABLE 1: Inhibition effect of Gecko-contained serum on HepG2 by MTT assay (mean  $\pm$  SD,  $n = 12$ ).

Groups	Dose mg/mL	24 h		48 h		72 h	
		A	IR%	A	IR%	A	IR%
NS		0.42 $\pm$ 0.12	—	0.63 $\pm$ 0.02	—	0.95 $\pm$ 0.10	—
5-FU	1.3	0.20 $\pm$ 0.03*	53	0.14 $\pm$ 0.04*	77	0.07 $\pm$ 0.02**	92
	3	0.16 $\pm$ 0.06*	63	0.13 $\pm$ 0.03**	76	0.08 $\pm$ 0.10**	91
	1.5	0.24 $\pm$ 0.01*	42	0.26 $\pm$ 0.01**	57	0.27 $\pm$ 0.04**	78
GCPs	1	0.29 $\pm$ 0.02*	30	0.31 $\pm$ 0.03**	46	0.38 $\pm$ 0.06**	69
	0.75	0.32 $\pm$ 0.02*	23	0.37 $\pm$ 0.04**	31	0.39 $\pm$ 0.04**	58
	0.375	0.37 $\pm$ 0.02*	12	0.40 $\pm$ 0.02	25	0.45 $\pm$ 0.01**	43

\* $P < 0.05$ , \*\* $P < 0.01$  versus control.

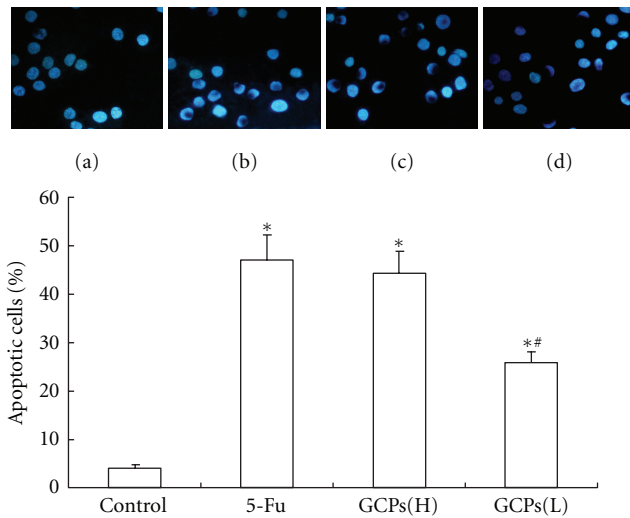


FIGURE 1: Hoechst-stained nuclei of apoptotic myocytes were analyzed morphologically and were expressed as the percentage of total nuclei (magnification  $\times 400$ ). (a) NS control group; (b) 1.3 mg/mL 5-Fu; (c) GCPs (H): 1.6 mg/mL GCPs; (d) GCPs(L): 0.8 mg/mL GCPs. The percentage rate of apoptotic cells was presented in bar graph. The data were expressed as the mean  $\pm$  SEM. \* $P < 0.05$  versus control. \*\* $P < 0.05$  versus 5-FU.

**2.4. Statistical Analysis.** Unless otherwise indicated, all experiments were repeated at least three times and the differences were determined by the two-tailed Student's  $t$ -test. When the statistical differences between more than two groups were analyzed, a one-way ANOVA followed by Dunnett's test was performed. Results were presented as means  $\pm$  standard deviations (SDs) of three independent experiments.  $P$ -values  $< 0.05$  were considered statistically significant.

### 3. Results

**3.1. GCPs Inhibit HepG2 Cell Proliferation.** Compared with the control group, the growth of HepG2 cells treated with GCPs was significantly inhibited in a time- and dose-dependent manner ( $P < 0.05$ ; Table 1). After 48 h treatment, the inhibitory rates for GCPs ranged from 12%–63%.

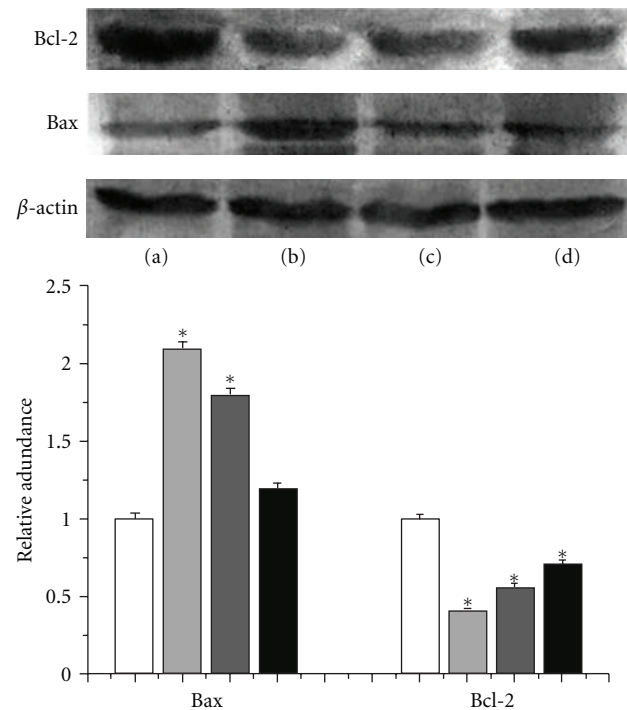


FIGURE 2: Effects of GCPs on the expressions of bcl-2 and bax protein in HepG2 cells. Lane (a): control; Lane (b): 5-Fu (1.3 mg/mL); Lane (c): GCPs (1.6 mg/mL); Lane (d): GCPs (0.8 mg/mL). \* $P < 0.05$  versus Control.

**3.2. GCPs Induce Apoptosis in HepG2 Cells.** As shown in Figure 1. The NS group did not display any morphological features of apoptosis (Figure 1(a)). The typical changes associated with apoptotic cells appeared in GCPs-treated cells after 48 h incubation, the nuclei of apoptotic cells showed significant apoptosis in 1.6 and 0.8 mg/mL GCPs-treated cells (Figures 1(c) and 1(d)).

**3.3. GCPs Decrease the Bcl-2 and Bax Ratio in HepG2 Cells.** As shown in Figure 2, compared to the NS group, bcl-2 protein expression decreased in the 1.6 mg/mL or 0.8 mg/mL GCPs-treated group; however, bax protein expression was increased in 1.6 mg/mL or 0.8 mg/mL GCPs. Therefore, GCPs increased the bcl-2/bax ratio in HepG2 cells.

TABLE 2: Inhibitory effects of Gecko on transplanted H22 mice (mean  $\pm$  SD,  $n = 10$ ).

Groups	Dosage (mg/kg)	Tumor weight (g)	Inhibitory rate (%)
NS	0	2.2 $\pm$ 0.45	—
ADR	2	1.0 $\pm$ 0.38	53.8**
GCPs (H)	80	0.98 $\pm$ 0.6	54.6**
GCPs (M)	40	1.6 $\pm$ 0.41	24.8*
GCPs (L)	20	1.8 $\pm$ 0.85	16.6

\*  $P < 0.05$ , \*\*  $P < 0.01$  versus control.

**3.4. GCPs Exert Antitumor Effects on H22 Xenograft Tumors in Mice.** As shown in Table 2, compared to NS groups, the tumors weight decreased in the GCPs and ADR groups ( $P < 0.01$ ; Table 2). The tumor weights in the GCPs groups (80, 40, and 20 mg/kg) were not significantly different to the ADR group (1.0  $\pm$  0.38 g). The tumor inhibitory rates of the ADR and GCPs groups were 53.8%, 54.6%, and 24.8%, respectively.

**3.5. GCPs Improve the Immune Function of Mice Bearing H22 Xenograft Tumors.** As shown in Table 3, the white blood cell count, spleen index, and thymus index of mice in the 80 mg/kg GCPs and ADR groups were significantly lower than the NS group ( $P > 0.05$ ); however, there was no significant difference between the NS group and the 40 mg/mL or 20 mg/mL GCPs groups. Compared to the NS group, the body weight of the ADR group was significantly decreased ( $P < 0.01$ ; Table 3).

**3.6. GCPs Downregulate Expression of VEGF in H22 Xenograft Tumors.** As shown in Figure 3, VEGF expression significantly increased in NS group, GCPs decreased VEGF protein expression in a dose-dependent manner in xenograft tumor tissues.

**3.7. GCPs Reduce the Serum Levels of TNF- $\alpha$  and IL-6 in Mice Bearing H22 Xenograft Tumors.** As shown in Table 4, the serum levels of TNF- $\alpha$  and IL-6 were lower in the GCPs groups and ADR group than the NS group ( $P < 0.05$ ). The serum levels of TNF- $\alpha$  and IL-6 in the GCPs groups and ADR group were not significantly different.

## 4. Discussion

A growing number of studies have revealed that the small-molecule peptides, extracted from animals, exert antitumor effects [3, 4]. In recent years, researchers have emphasized to the antitumor activity of natural polypeptide extracts. Natural peptides can be extracted from animals, microorganisms, and other organisms using special extraction and separation processes, and *in vitro* or *in vivo* experiments have demonstrated that many of these substances have significant antitumor activity [3, 4]. Compared with conventional chemotherapy and radiotherapy, polypeptides with natural antitumor activity have the advantages of a low-

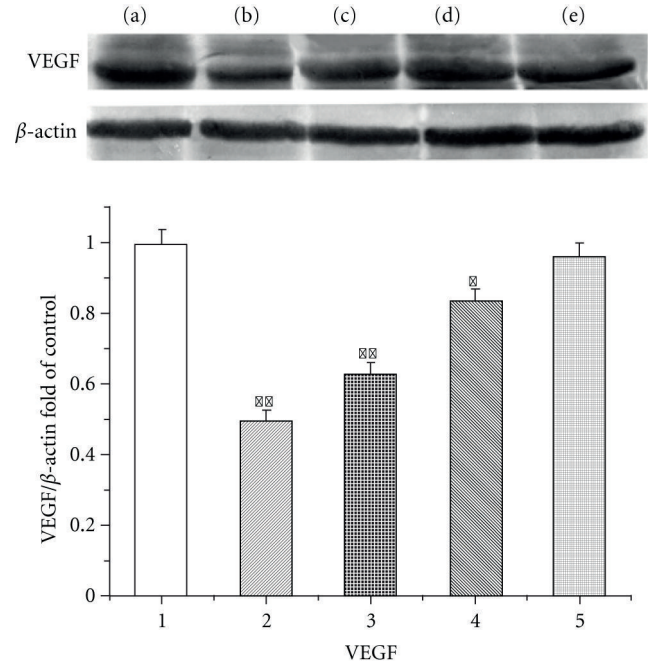


FIGURE 3: Effects of GCPs on the expression of VEGF protein in the tumor tissue. Lane (a): control; Lane (b): ADR (2 mg/kg); Lane (c): GCPs (80 mg/kg); Lane (d): GCPs (40 mg/kg); Lane (e): GCPs (20 mg/kg). \*  $P < 0.05$ , \*\*  $P < 0.01$  versus Control; #  $P < 0.01$  versus ADR.

molecular weight, high activity, few side effects, and they do not usually induce drug resistance easily [3, 4]. The aim of this study was to further separate and purify Gecko alcohol extract (GAE) to obtain Gecko crude peptides (GCPs), in order to investigate the antitumor effect and mechanism of action of GCPs on HepG2 cells *in vitro* and *in vivo*.

In this study, we observed that GCPs inhibited the proliferation of HepG2 cells in a time, and dose-dependent manner with a half-maximal inhibitory concentration ( $IC_{50}$ ) of 1.2 mg/mL. Two major apoptotic signaling pathways are the death receptor (extrinsic) and mitochondrial (intrinsic) pathways, which can crosstalk to each other [16, 19–23]. The bcl-2 family members appear to regulate the commitment to survive or die by controlling the integrity of mitochondrial membrane [24]. HepG2 cells treated with GCPs displayed the morphological features of apoptosis, including dense, strong blue fluorescence under fluorescence microscopy. Additionally, GCPs at a concentration of 0.8 and 1.6 mg/mL increased the bcl-2/bax ratio in HepG2 cells. These results indicate that GCPs can induce apoptosis in HepG2 cells *in vitro* by increasing the bcl-2/bax ratio. Therefore, GCPs are a potentially effective antitumor agent.

This study also demonstrated that GCPs could significantly inhibit the growth of H22 xenograft tumors *in vivo* and were similarly effective to ADR. GCPs also had beneficial effects on the immune system of the mice-bearing tumors and did not affect the weight of the mice, indicating that

TABLE 3: Influence of Gecko on immune organs of transplanted H22 in mice (mean  $\pm$  SD,  $n = 10$ ).

Groups	Dosage (mg/kg)	Body weight (g)	White blood cell count ( $\times 10^9/L$ )	Spleen index (mg/10 g)	Thymus index (mg/10 g)
NS	0	29.35 $\pm$ 3.2	7.86 $\pm$ 2.1	81.3 $\pm$ 12.5	14.7 $\pm$ 0.5
ADR	2	23.18 $\pm$ 3.6**	6.04 $\pm$ 2.3	65.3 $\pm$ 11.8	9.4 $\pm$ 0.4**
GCPs (H)	80	26.13 $\pm$ 2.5*	9.88 $\pm$ 0.8*	117.1 $\pm$ 10.6*	21.6 $\pm$ 0.4**
GCPs (M)	40	26.71 $\pm$ 1.8	8.11 $\pm$ 3.16	99.8 $\pm$ 15.4	20.9 $\pm$ 0.7**
GCPs (L)	20	27.68 $\pm$ 2.7	7.06 $\pm$ 1.64	92.7 $\pm$ 11.6	17.5 $\pm$ 0.6*

\*  $P < 0.05$ , \*\*  $P < 0.01$  versus control.

TABLE 4: Effects of GCPs on the expressions of TNF- and IL-6 protein in the tumor tissue.

Groups	Dosage (mg/kg)	TNF- $\alpha$ (pg/mL)	IL-6 (pg/mL)
NS	0	68.51 $\pm$ 2.43	75.83 $\pm$ 1.74
ADR	2	32.15 $\pm$ 3.24**	48.36 $\pm$ 4.32**
GCPs (H)	80	34.62 $\pm$ 4.51**	50.78 $\pm$ 5.34**
GCPs (M)	40	46.81 $\pm$ 6.34**	56.37 $\pm$ 3.61**
GCPs (L)	20	60.66 $\pm$ 7.83*	63.28 $\pm$ 3.23**

\*\*  $P < 0.01$ , \*  $P < 0.05$  versus control.

GCPs are nontoxic with few side effects. Additionally, GCPs significantly decreased the VEGF protein expression levels in the xenograft tumors and the lowered the serum levels of TNF- $\alpha$  and IL-6, suggesting that GCPs can inhibit tumor angiogenesis and tumor growth. Taken together, this study illustrates that GCPs exert a significant anticancer effect *in vivo*.

## Authors Contribution

J.-G. Wang and Y. Song contributed equally to this work; J.-G. Wang and Y. Song designed the research; J.-G. Wang and Y. Song wrote the paper.

## Acknowledgments

This study was supported by Medical Science and Technology Research Project of Henan Province, China, no. 200903109.

## References

- [1] B. H. Y. Yeung, K. Y. Wong, M. C. Lin et al., "Chemosensitisation by manganese superoxide dismutase inhibition is caspase-9 dependent and involves extracellular signal-regulated kinase 1/2," *British Journal of Cancer*, vol. 99, no. 2, pp. 283–293, 2008.
- [2] T. Tanaka, S. Toujima, T. Utsunomiya, K. Yukawa, and N. Umehashi, "Experimental characterization of recurrent ovarian immature teratoma cells after optimal surgery," *Oncology Reports*, vol. 20, no. 1, pp. 13–23, 2008.
- [3] J. L. Zhang, H. M. Wen, and D. J. Sun, "Purification and anti-tumor effects of a small peptide from snake venom of *Gloydius saxatilis*," *Chinese Journal of Biochemical Pharmaceutics*, vol. 30, no. 4, pp. 217–220, 2009.
- [4] W. D. Zhang, Y. Y. Zhang, C. X. Wang et al., "Effect of polypeptide extract from scorpion venom on tumor growth and cellular immunity in rats with W256 sarcomatoma," *Journal of Shandong University*, vol. 45, no. 3, pp. 286–289, 2007.
- [5] F. Zhao and P. X. Liu, "Progress of study on action mechanisms of TCM in anti-tumor and preventing metastasis of tumor," *Zhongguo Zhongxiyi Jiehe Zazhi*, vol. 27, no. 2, pp. 178–181, 2007.
- [6] Y. H. He, "General survey of traditional Chinese medicine and Western medicine researches on tumor metastasis," *Chinese Journal of Integrative Medicine*, vol. 12, no. 1, pp. 75–80, 2006.
- [7] S. F. Zhang, Z. Chen, and B. Li, "Progress on research and application of traditional Chinese medicine in intervention treatment of primary liver carcinoma," *Zhongguo Zhongxiyi Jiehe Zazhi*, vol. 26, no. 8, pp. 759–763, 2006.
- [8] J. X. Yang and X. M. Wang, "Progress in studies on anti-hepatoma effect of traditional Chinese medicine by adjusting immune function," *Zhongguo Zhongyao Zazhi*, vol. 32, no. 4, pp. 281–284, 2007.
- [9] F. Liu, J. G. Wang, S. Y. Wang, Y. Li, Y. P. Wu, and S. M. Xi, "Antitumor effect and mechanism of Gecko on human esophageal carcinoma cell lines in vitro and xenografted sarcoma 180 in Kunming mice," *World Journal of Gastroenterology*, vol. 14, no. 25, pp. 3990–3996, 2008.
- [10] W. Xiaolan and H. Hengyou, "Study on the antitumor effects and synergism and attenuation effects of Gecko Alcohol Extract," *Journal of Chinese Medicinal Materials*, vol. 33, no. 8, pp. 1213–1216, 2010.
- [11] J. X. Yang and X. M. Wang, "Progress study and research on treating tumor of Gecko," *Chinese Journal of Digestion*, vol. 14, pp. 2428–2431, 2006.
- [12] B. D. Wu, "Treatment of 105 cases of esophagus tumor by compound recipe of Gecko," *Zhongguo Zhongxiyi Jiehe Za Zhi*, vol. 19, p. 502, 1999.
- [13] P. Song, X. M. Wang, and S. Xie, "Experimental study on mechanisms of lyophilized powder of fresh gekko *Chinenis* in inhibiting H22 hepatocarcinoma angiogenesis," *Zhongguo Zhongxiyi Jiehe Zazhi*, vol. 26, no. 1, pp. 58–62, 2006.
- [14] J. Fu, H. Huang, J. Liu, R. Pi, J. Chen, and P. Liu, "Tanshinone IIA protects cardiac myocytes against oxidative stress-triggered damage and apoptosis," *European Journal of Pharmacology*, vol. 568, no. 1–3, pp. 213–221, 2007.
- [15] L. Wang, J. Mao, G. H. Zhang, and M. J. Tu, "Nano-cerium-element-doped titanium dioxide induces apoptosis of Bel 7402 human hepatoma cells in the presence of visible light," *World*

- Journal of Gastroenterology*, vol. 13, no. 29, pp. 4011–4014, 2007.
- [16] S. L. Yuan, Y. Q. Wei, X. J. Wang, F. Xiao, S. F. Li, and J. Zhang, “Growth inhibition and apoptosis induction of tanshinone II-A on human hepatocellular carcinoma cells,” *World Journal of Gastroenterology*, vol. 10, no. 14, pp. 2024–2028, 2004.
- [17] X. Zhen, J. Cen, Y. M. Li, F. Yan, T. Guan, and X. Z. Tang, “Cytotoxic effect and apoptotic mechanism of tanshinone A, a novel tanshinone derivative, on human erythroleukemic K562 cells,” *European Journal of Pharmacology*, vol. 667, pp. 129–135, 2011.
- [18] T. Kakita, K. Hasegawa, T. Morimoto, S. Kaburagi, H. Wada, and S. Sasayama, “p300 Protein as a coactivator of GATA-5 in the transcription of cardiac-restricted atrial natriuretic factor gene,” *Journal of Biological Chemistry*, vol. 274, no. 48, pp. 34096–34102, 1999.
- [19] W. J. Chen, Y. T. Huang, M. L. Wu, T. C. Huang, C. T. Ho, and M. H. Pan, “Induction of apoptosis by vitamin D<sub>2</sub>, ergocalciferol, via reactive oxygen species generation, glutathione depletion, and caspase activation in human leukemia cells,” *Journal of Agricultural and Food Chemistry*, vol. 56, no. 9, pp. 2996–3005, 2008.
- [20] J. Li, X. Xia, H. Nie, M. A. Smith, and X. Zhu, “PKC inhibition is involved in trichosanthin-induced apoptosis in human chronic myeloid leukemia cell line K562,” *Biochimica et Biophysica Acta*, vol. 1770, no. 1, pp. 63–70, 2007.
- [21] S. Y. Park, H. C. Yang, J. Y. Moon et al., “Induction of the apoptosis of HL-60 promyelocytic leukemia cells by *Eurya emarginata*,” *Cancer Letters*, vol. 205, no. 1, pp. 31–38, 2004.
- [22] G. S. Zhang, C. Q. Tu, G. Y. Zhang, G. B. Zhou, and W. L. Zheng, “Indomethacin induces apoptosis and inhibits proliferation in chronic myeloid leukemia cells,” *Leukemia Research*, vol. 24, no. 5, pp. 385–392, 2000.
- [23] X. Zhen, Y. M. Li, W. R. Fang, F. Yan, J. Cen, and L. S. Mao, “Study on the effects of tanshinone derivatives on growth inhibition and apoptosis induction in human erythroleukemia cell line K562,” *Chinese Pharmacological Bulletin*, vol. 24, no. 7, pp. 964–968, 2008.
- [24] S. Cory and J. M. Adams, “The BCL2 family: regulators of the cellular life-or-death switch,” *Nature Reviews Cancer*, vol. 2, no. 9, pp. 647–656, 2002.